

# Development of rotational rheometers by introducing UVP

Takahisa Shiratori, Ichiro Kumagai, Yuji Tasaka, Yuichi Murai and Yasushi Takeda  
 Graduate School of Engineering, Hokkaido University, N13-W8, Kita-ku, Sapporo, 060-8628, Japan  
 t.shiratori@ring-me.eng.hokudai.ac.jp

Most of commercial rheometers have thin measuring section to ignore spatial distribution of shear rate. The objective of this research is obtaining more information about rheological properties in shorter time by taking into account the spatial distribution of the shear rate. Velocity fields of Newtonian and non-Newtonian fluids in a rotating cylinder are measured by a UVP-Duo. The velocity fields are converted to two velocity components on the two-dimensional plane (2D2C) by a method we established. Effects of measurement errors of the UVP on the 2D2C velocity field through the conversion method are assessed quantitatively by introducing numerical simulation. The result shows that measurement errors are amplified near the wall of the cylinder. Applications of the velocity fields for rheometry are suggested. In the suggested rheometry, a strain range of linear viscoelasticity can be detected without changing the oscillation amplitude. Shear rate dependent viscosity can also be measured without changing the rotation speed.

**Keywords:** Rheometry, rheology, rotating cylinder, multi velocity components, polyacrylamide solution

## 1 INTRODUCTION

Nowadays foods are required not only to supply nutrients but to provide enjoyment through new flavors and textures. Physical factors, for example hardness, viscosity and shape, affect feeling of the people as much as chemical factors, for example sweetness, bitterness and fragrance. The physical factors are quantitatively evaluated by introducing rheological properties such as viscosity, storage modulus and loss modulus. These properties are measured by equipment called rheometer. Furthermore, rheometers are utilized in industries other than food industry. For example, rheological properties given by rheometers are helpful for quality control in polymer industry.

Existing commercial rheometers have two problems: one is a limitation of test fluids, and the second is a long measurement time. These rheometers generally have thin measuring section in order to ignore spatial distribution of shear rate in test fluids. Thus they cannot measure properties of fluids with larger ingredients than the thickness of measurement sections: for instance juice with fruit pulps. The long measurement time is also owing to the thin measuring section. Because spatial distribution of shear rate is ignored, one rotational speed corresponds to one shear rate. By taking into account spatial distribution of shear rate, viscosity under a range of shear rate is obtained from one rotational speed measurement.

Nowadays it is possible to take into account shear rate distribution with field velocimetry e.g. UVP. Thus a rheometer with a thick measurement section can be designed while taking into account shear rate distribution. Viscosity distribution due to shear rate dependent viscosity is also obtained. It means that the relationship between shear rate and

viscosity is measured simultaneously. Actually a system named UVP-PD [1] enabled to measure shear rate dependent viscosity. As described above, problems of commercial rheometers can be overcome with UVP.

According to this strategy we have developed a novel rheometry for viscoelastic [2] and multiphase [3] flows based on UVP. The rheometry requires obtaining two velocity components on two-dimensional plane (2D2C), and it has been achieved with some assumption. One of critical factors for relevance of the rheometry is effects from measurement errors of UVP on 2D2C velocity field. Thus the assessment of the error conversion is demonstrated by introducing numerical simulation as the first topic of this paper. Then applications of 2D2C velocity field to rheometry are suggested. The applications can measure shear rate dependent viscosity and perform linearity check in oscillation test simultaneously.

## 2 EXPERIMENT

### 2.1 Experimental apparatus

Figure 1 shows the experimental apparatus. It consists of a cylinder, a rectangular container, stepping motor and UVP-Duo as shown in Fig. 1 (a). The cylinder is filled with a test fluid: silicone oil (KF96-1000cs, Shin-Etsu Chemical) or 1.0 wt% polyacrylamide (PAA, AP805C, DiaNitrix) solution. The silicone oil is regarded as Newtonian fluid whose viscosity  $\eta$  and density  $\rho$  are 0.970 Pa·s and  $0.967 \times 10^3 \text{ kg/m}^3$  respectively. The PAA solution has shear rate dependent viscosity and viscoelasticity. The detail of these properties is summarized in section 2.3. The rectangular container is partially filled with water to introduce ultrasonic pulse into the cylinder without reflection. The height  $H$  and the diameter  $D$  of the cylinder are

300 mm and 154 mm respectively as shown in Fig. 1(b). An ultrasound transducer is fixed nearby the cylinder with 150 mm in height from the bottom of the cylinder. The rotation of the cylinder is controlled by a stepping motor for being oscillatory rotation. The velocity of the wall of the cylinder is described as Eqs. (1) and (2).

$$u_{wall}(t) = U_{wall} \sin 2\pi ft. \quad (1)$$

$$U_{wall} = \pi f D \theta. \quad (2)$$

In this experiment, frequency of the rotation  $f$  is 0.5 Hz, and rotation angle  $\theta$  is  $\pi$ . Then the maximum velocity of the cylinder  $U_{wall}$  is 760 mm/s. Time resolution  $\Delta t$ , channel distance  $\Delta x$  and velocity resolution  $\Delta u$  are set at 34 msec, 0.367 mm and 0.625 mm/s respectively.

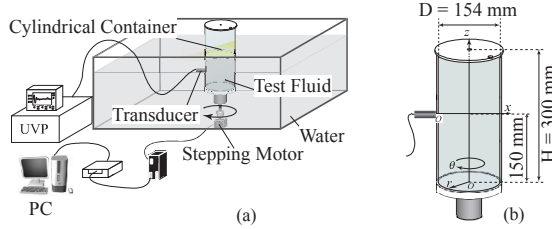


Figure 1: Diagram of (a) the overview of the experimental apparatus (b) the detail of the cylinder

## 2.2 Conversion method from $u_x$ to $u_\theta$ and $u_r$

Tangential and radial velocity components,  $u_\theta$  and  $u_r$ , respectively, are necessary to obtain rheological properties from velocity information. Thus we developed a method to determine  $u_\theta$  and  $u_r$  from a velocity profile on the measurement line  $u_x$ . Figure 2 shows a top view of the cylinder. Measurement line lies on 7.0 mm from the rotation axis of the cylinder. Under the assumption of axial symmetry,  $u_{x+}$  and  $u_{x-}$  in Fig. 2 are velocity information about the same velocity vector. Thus  $u_\theta$  and  $u_r$  are calculated from  $u_{x+}$  and  $u_{x-}$  by Eqs. (3) and (4) respectively.

$$u_\theta = \frac{u_{x+} + u_{x-}}{2 \cos \alpha}. \quad (3)$$

$$u_r = \frac{u_{x+} - u_{x-}}{2 \cos \alpha}. \quad (4)$$

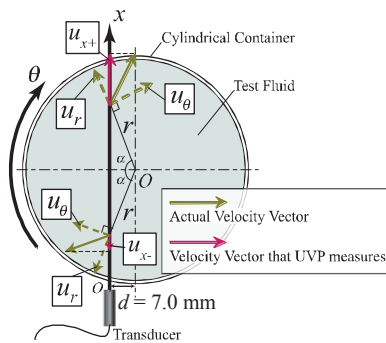


Figure 2: Top view of the cylinder

## 2.3 Properties of 1.0 wt% PAA solution

The PAA solution used for this experiment is one of popular non-Newtonian fluids for laboratory experiment. Rheological properties of the PAA solution, shear rate dependent viscosity and viscoelasticity, were measured with a commercial rheometer (Bohlin CVO, Malvern Instruments). The measured viscosity is plotted in Fig. 3 (a) as a function of shear rate. The shear viscosity decreases with the increase of shear rate: namely the PAA solution is a shear thinning fluid. Figure 3 (b) shows the relationship between the measured dynamic moduli, storage modulus  $G'$  and loss modulus  $G''$ , and the applied frequency. Amplitude of stress is set as 1.0 Pa. In the frequency range of Fig. 3 (b), including the experimental condition introduced to this experiment ( $f = 0.5$  Hz),  $G'$  is always larger than  $G''$ . It is expected that the contribution from elasticity to stress is larger than that from viscosity under the experimental condition.

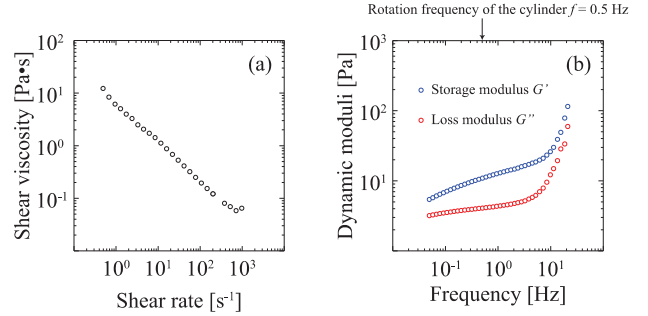


Figure 3: The relationship between (a) viscosity and shear rate, and (b) dynamic moduli and frequency

## 3 VELOCITY FIELDS

Spatio-temporal distributions of the velocity components are shown in Figs. 4 and 5. Spatial (horizontal) axis and temporal (vertical) axis are normalized by radius of the cylinder  $D/2$  and inverse of the oscillation frequency  $1/f$  respectively. Velocity components are normalized by the maximum velocity of the wall  $U_{wall}$ . Radial velocity component  $u_r$  and tangential velocity component  $u_\theta$  are indicated as (a) and (b) in the figures, respectively. In the region of  $r < 7.0$  mm ( $2r/D < 0.09$ ), velocity cannot be measured because the measurement line doesn't take corresponding radial positions with this region (see Fig. 2). The distributions in Figs. 4 and 5 are obtained in case of the silicone oil and the PAA solution respectively. In both cases  $u_\theta$  is about ten times larger than  $u_r$ . Thus the tangential velocity component  $u_\theta$  is mainly discussed in the following sections.

## 4 EVALUATION OF ERROR CONVERSION

### 4.1 Method

The original velocity distribution obtained by UVP includes measurement errors. The errors

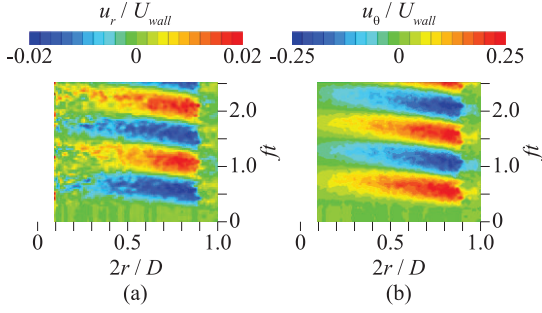


Figure 4: Spatio-temporal distribution of (a) radial velocity component and (b) tangential velocity component in silicone oil

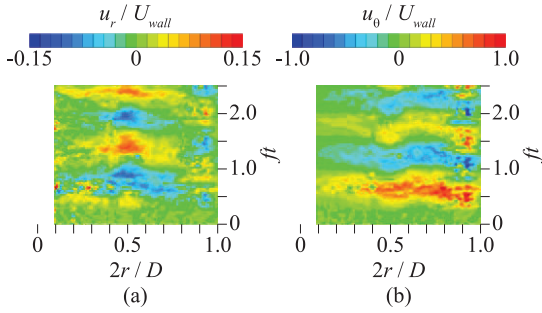


Figure 5: Spatio-temporal distribution of (a) radial velocity component and (b) tangential velocity component in PAA solution

affect the result through the conversion method from  $u_x$  to  $u_\theta$  and  $u_r$  we developed. Conversion characteristics of the errors were evaluated quantitatively by performing our conversion method for the result of a numerical simulation. Equation of motion for Newtonian fluids in the tangential direction, Eq. (5), is solved numerically to obtain a spatio-temporal distribution of  $u_\theta$  component.

$$\frac{\partial u_\theta}{\partial t} = \eta \left( \frac{\partial^2 u_\theta}{\partial r^2} + \frac{1}{r} \frac{\partial u_\theta}{\partial r} - \frac{u_\theta}{r^2} \right). \quad (5)$$

The obtained  $u_\theta$  distribution is regarded as correct velocity distribution  $u_{cor}(r,t)$ . This velocity distribution is rearranged and projected on the measurement line  $x$ :

$$u_{cor}(x,t) = u_{cor}(r,t) \cos \alpha \quad (6)$$

where  $\alpha$  is the center angle shown in Fig. 2. The velocity distribution measured by UVP,  $u_{UVP}(x,t)$ , can be expressed as

$$u_{UVP}(x,t) = u_{cor}(x,t) + Er_g(x,t), \quad (7)$$

where  $Er_g(x,t)$  means that the measurement error produced by the UVP itself because of a measurement of a reflection echo or detection of Doppler shift frequency.  $Er_g(x,t)$  is assumed to obey a normal distribution. The standard deviation of the normal distribution  $\sigma_g$  is varied from 0 to  $5.0\Delta u$ . Finally  $u_{UVP}(x,t)$  is converted to a velocity distribution on  $r$  axis by Eq. (8) derived from Eq. (3).

$$u_{UVP}(r,t) = \frac{u_{UVP}(x+,t) + u_{UVP}(x-,t)}{2 \cos \alpha}. \quad (8)$$

A difference between  $u_{UVP}(r,t)$  and  $u_{cor}(r,t)$  is regarded as an error distribution on  $u_{UVP}(r,t)$ . This error distribution is represented by  $Er(r,t)$ :

$$Er(r,t) = u_{UVP}(r,t) - u_{cor}(r,t). \quad (9)$$

In other words,  $Er_g(x,t)$  is converted to  $Er(r,t)$  by our conversion method. Thus the relationship between them means error conversion characteristics of our conversion method. Standard deviation of  $Er(r,t)$  is represented by  $\sigma$ , and compared with  $\sigma_g$ .

#### 4.2 The results of the evaluation

At first, standard deviation  $\sigma$  was calculated for time series of  $Er$  on each  $r$  position in order to clarify spatial distribution of  $\sigma/\sigma_g$  ratio. The  $\sigma/\sigma_g$  ratio means how much measurement errors are amplified by the conversion. The  $\sigma/\sigma_g$  ratio for  $\sigma_g = 5.0\Delta u$  is plotted in Fig. 6 (a) as a function of spatial position. Near the center of the cylinder, around  $2r/D = 0.2$ ,  $\sigma$  approximately equals to  $\sigma_g$ . On the other hand, near the wall of the cylinder,  $\sigma$  is as 5 times large as  $\sigma_g$ . Therefore Fig. 6 (a) means that the measurement error is amplified especially near the wall of the cylinder. This amplification occurs because the center angle  $\alpha$  is large near the wall thus the division by  $\cos \alpha$  in Eq. (8) amplifies errors.

The relationship between  $\sigma$  and  $\sigma_g$  is shown in Fig. 6 (b). The relation means how errors on  $r$ - $t$  velocity distribution changes depending on measurement errors of UVP. In Fig. 6 (b), spatial distribution of  $\sigma$  is not considered: a parent population of  $\sigma$  is all errors on spatio-temporal distribution. As  $\sigma_g$  increases,  $\sigma$  converges to the primary function shown by the green line. It means that if  $\sigma_g$  is large enough,  $\sigma$  is a constant multiple of  $\sigma_g$ . On the other hand, the primary function cannot explain the relationship between  $\sigma_g$  and  $\sigma$  in the region of smaller  $\sigma_g$ . Figure 6 (b) shows that  $\sigma$  has a certain value shown by the blue line when  $\sigma_g$  equal zero. It means that  $r$ - $t$  velocity distribution has errors even if measurement errors of UVP do not exist.

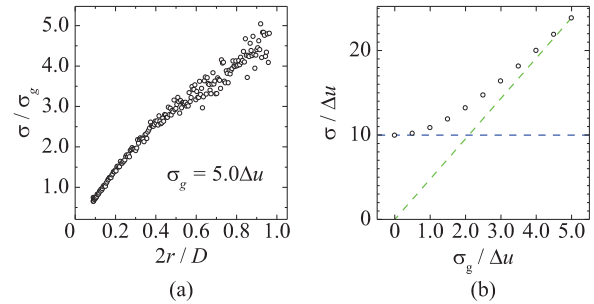


Figure 6: Standard deviation of errors on  $r$ - $t$  velocity distribution converted from  $x$ - $t$  velocity distribution (a) Spatial distribution (b) Dependency on standard deviation of errors on  $x$ - $t$  velocity distribution

## 5 THEORIES FOR RHEOMETRY

In this section, two theories to apply 2D2C velocity field for rheometry is suggested: the first one is an evaluation of viscoelasticity under oscillatory rotations, and the second one is a measurement of shear rate dependent viscosity under steady rotations. In both cases, the experimental apparatus have to be improved to measure shear stress on the wall. Additionally fixed inner cylinder is necessary for the steady rotation test to prevent a rigid rotation.

### 5.1 Storage and loss moduli

By measuring a shear stress on the wall of the cylinder, strain dependency of  $G'$  and  $G''$  can be measured simultaneously. Here a process to obtain  $G'$  and  $G''$  is explained. The momentum conservation law in the rotating cylinder for  $\theta$  component is described by Eq. (10) under the assumption of uniformity for  $\theta$  and  $z$  direction.

$$\rho \left( \frac{\partial u_\theta}{\partial t} + u_r \frac{\partial u_\theta}{\partial r} + \frac{u_r u_\theta}{r} \right) = \frac{2\tau}{r} + \frac{\partial \tau}{\partial r}. \quad (10)$$

Information in the left-hand side of Eq. (10) is obtained by the conversion technique suggested in this report. Thus spatio-temporal stress distribution  $\tau(r,t)$  is obtained by solving Eq. (10) numerically. Furthermore shear rate distribution  $\dot{\gamma}$  and strain distribution  $\gamma$  are obtained from velocity distribution.

$$\dot{\gamma}(r,t) = \frac{\partial u_\theta}{\partial r} - \frac{u_\theta}{r}. \quad (11)$$

$$\gamma(r,t) = \int_0^t \dot{\gamma}(r,T) dT. \quad (12)$$

In order to obtain  $G'$  and  $G''$ , the cylinder is controlled to rotate oscillatory. If the flow phenomenon is under the linear viscoelastic regime, a time variation of the three quantities,  $\gamma$ ,  $\dot{\gamma}$  and  $\tau$ , satisfy,

$$\gamma(r,t) = \gamma_0(r) \cos 2\pi f t, \quad (13)$$

$$\dot{\gamma}(r,t) = -\dot{\gamma}_0(r) \sin 2\pi f t, \quad (14)$$

$$\tau(r,t) = \tau_0(r) \cos\{2\pi f t + \delta(r)\}, \quad (15)$$

where  $\gamma_0$ ,  $\dot{\gamma}_0$  and  $\tau_0$  are amplitudes of strain, shear rate and stress, respectively. Eqs. (13) and (15) mean that the spatial distribution of phase difference  $\delta$  is obtained by comparing  $\dot{\gamma}(r,t)$  and  $\tau(r,t)$ . Then a spatial distributions of  $G'$  and  $G''$  are obtained as

$$G'(r) = \frac{\tau_0(r)}{\gamma_0(r)} \cos \delta(r), \quad (16)$$

$$G''(r) = \frac{\tau_0(r)}{\gamma_0(r)} \sin \delta(r). \quad (17)$$

In these equations,  $G'$  and  $G''$  are described as the

functions of radial position  $r$ . These functions can be converted to functions of  $\gamma_0$  because the relationship between  $r$  and  $\gamma_0$  is given by Eq. (13). Consequently the relationship between  $G'$ ,  $G''$  and  $\gamma_0$  is obtained without changing an oscillation amplitude.

### 5.2 Non-Newtonian viscosity

With a fixed inner cylinder, a rigid rotation is prevented and shear rate dependent viscosity can also be measured. In steady rotation test, Eq. (10) is simplified to Eq. (18) because the term of time derivative can be ignored.

$$\rho \left( u_r \frac{\partial u_\theta}{\partial r} + \frac{u_r u_\theta}{r} \right) = \frac{2\tau}{r} + \frac{\partial \tau}{\partial r}. \quad (18)$$

Spatial distribution of stress  $\tau(r)$  is obtained from Eq. (18) as is the case in Eq. (10), and spatial distribution of shear rate  $\dot{\gamma}(r)$  is also obtained from Eq. (11). Then the spatial distribution of viscosity is obtained by

$$\eta(r) = \frac{\tau(r)}{\dot{\gamma}(r)}. \quad (19)$$

The spatial distribution can be converted to shear rate dependency by considering Eq. (11). Therefore the technique to obtain 2D2C velocity distribution enables to measure shear rate dependent viscosity without changing a rotation speed.

## 6 CONCLUSION

Velocity fields of a silicone oil and polyacrylamide (PAA) solution in the rotating cylinder were measured by UVP. Under the assumption of axial symmetry, two velocity components,  $u_\theta$  and  $u_r$ , were obtained on  $r$  axis (2D2C velocity field). The error conversion characteristics were assessed quantitatively. As the result, it was clarified that measurement errors are amplified especially near the wall of the cylinder. By summarizing the works mentioned above, ultrasonic rotational rheometer was suggested. In this system, it is possible to detect a strain range of linear viscoelastic region from an oscillation test without strain sweeping. Shear rate dependent viscosity can also be measured without changing the rotational speed by installing a fixed inner cylinder. In order to realize these systems, shear stress has to be measured on the wall of the inner or outer cylinder.

## REFERENCES

- [1] Wiklund J *et al.* : Methodology for in-line rheology by ultrasound Doppler velocity profiling and pressure difference techniques, *Chem. Eng. Sci.*, 62 (2007), 4277-4293.
- [2] Furuya N *et al.* : Development of Rheometry based on UVP for visco-elastic liquid, *Proc. of ISUD6*, (2008), 57-60.
- [3] Murai Y *et al.* : Ultrasound Doppler rheometry from spin response of viscoelastic and bubbly Liquids, *Proc. of ISUD7*, (2010), 9-12.